

PERFORMANCE ANALYSIS OF TRACKING FILTERS ACCORDING TO INPUT DATA PROCESSING

C. Carloni, M. Budoni, D. Cerutti-Maori, and J. Rosebrock

*Fraunhofer Institute for High Frequency Physics and Radar Techniques FHR, 53343 Wachtberg, Germany
Email: claudio.carloni@fhr.fraunhofer.de*

ABSTRACT

This paper investigates the performance of tracking filters for coherent radar systems according to the filter input data type. In the context of a real time implementation, the study examines the trade-off between the quality and the revisit rate of the input measurements. Three different kinds of input data are taken into consideration. In the first case, the raw observation vectors, available with a high refreshment rate, are directly used as input for the tracking filter. In the two other cases, the raw data are either averaged or filtered over a given time interval before feeding the tracking filter, thus reducing the overall revisit rate of the measurement update. Simulations are realized to study the tracking performance achieved with these different filter input data types. Finally, real data acquired by the Tracking and Imaging Radar (TIRA) are used to validate the findings.

Keywords: Tracking filter; Input data; Radar data processing.

1. INTRODUCTION

The TIRA system, developed and operated at Fraunhofer FHR, consists of a tracking radar and an imaging radar, which both use a 34 m parabolic antenna. During an observation, the antenna beam follows a space object and radar data are recorded. From these data, observation vectors are generated at different instants of time, which include the measurements of range, range rate, elevation and azimuth angles. These observation vectors can be used for various applications e.g. initial orbit determination and orbit determination. Real-time tracking filters are used to steer the antenna beam of the TIRA system to the selected space object in order to continuously track that object. These tracking filters can be fed with different types of data, which may affect the overall tracking performance of the system.

As a first option, the generated observation vectors can be directly fed to a tracking filter for orbit determination. According to the default pulse repetition frequency (PRF), which is about 30 Hz, a measurement update oc-

curs approximately every 33 ms.

In the context of a real-time implementation of an advanced tracking filter for the TIRA system, it could be beneficial to pre-process these data before feeding them to the tracking filter. This is done to reduce the revisit rate and to improve the estimation accuracy of the radar observables.

A second option consists in pre-processing the raw data through an averaging. As an example, the measurements are averaged over 30 pulses resulting in a measurement update around every second.

As a third possibility, a new local filtering technique has been recently developed to improve the accuracy of the observables at the cost of a higher computational load compared to a simple averaging [1]. A peculiarity of this technique is the estimation of an additional parameter, the range rate rate, i.e the second temporal derivative of the range. These filtered observation vectors are then used as input to the tracking filter.

The goal of this study is to understand which of these input data lead to the best performance of the tracking filter, which means the highest orbit determination accuracy. In particular, we want to investigate how the choice of the input data affects the filter efficiency by examining its convergence behaviour and accuracy. For instance, it is interesting to understand what is better between using raw observation vectors with a high measurement rate or more accurate observation vectors, estimated over several pulses, with a lower refreshment rate.

Another aspect to analyse deals with the implementation of a future real-time tracking filter. A trade-off between filter accuracy and computational load has to be found. This is the reason why, in this paper, as a second option of the three above-mentioned, we used a simple and fast averaging instead of the more complex one that is currently implemented in the TIRA system that works offline.

The TIRA system includes also an imaging radar. Since the imaging radar operates at a much higher frequency, the antenna footprint is much smaller compared to the one of the tracking radar. Thus, accurate tracking filters are needed to guarantee that the antenna beam of the imaging radar still illuminates the imaged space object. We considered the extended Kalman filter (EKF) for our study [2], also for a future perspective of real-time tracking. A first analysis of the performance of these input data is conducted through simulations. In particular, Section 2

shows some simulations that are performed in order to test the averaging and the new filtering technique. In addition, Section 3 verifies the same pre-processing techniques with real data through three observations of the French satellite Stella performed with the TIRA system in 2019. For each pass, the observation vectors are filtered according to the three above-mentioned options and used as input of the tracking filter.

Thanks to the accurate knowledge of the position of the satellite Stella over time from ephemerides, the results are presented in terms of residuals between the outputs of the EKF and the ephemerides. The exploitation of these residuals is the key to understand the performance of the tracking filter according to the input data processing. Lastly, Section 4 concludes the paper.

2. INVESTIGATED INPUT DATA

The goal of this section is to test, through simulations, the performance of the EKF according to the three different input data: raw data, averaged data and filtered data. The raw data are directly created from the simulation described in Section 2.1. Then, Section 2.2 and Section 2.3 investigate the averaging and the new local filtering technique, respectively.

2.1. Performed simulation

We simulated an observation of the French satellite Stella with the tracking radar of the TIRA system for a duration of 600 s. The satellite Stella was chosen as test object since we also have access to real data of the same satellite. The TLE used for the simulation is displayed in Table 1. Figure 1 shows the simulated parameters (range, range rate, azimuth and elevation) during the whole observation time. The range is contained in the interval between 1300 km and 2600 km and the elevation reaches a peak around 33 degrees near the point of closest approach. The raw data are created by adding white Gaussian-distributed noise (WGN) to these nominal measurements. The noise value depends on the accuracy of the different observation parameters, according to the corresponding signal-to-noise ratio (SNR). The lower the SNR, the higher the noise on the raw data. The SNR is kept constant for one simulation. It has to be mentioned that no error is introduced with the propagation of the state vector because the propagator used to simulate the trajectory is exactly the same as for the tracking filter.

2.2. Averaging

We averaged the raw data over a certain number of samples n_s , in order to generate new observation vectors, more accurate, but necessarily with a higher sampling time ($n_s \cdot 0.033$ s). Thus, a single observation vector is created out of n_s observation vectors. By assumption,

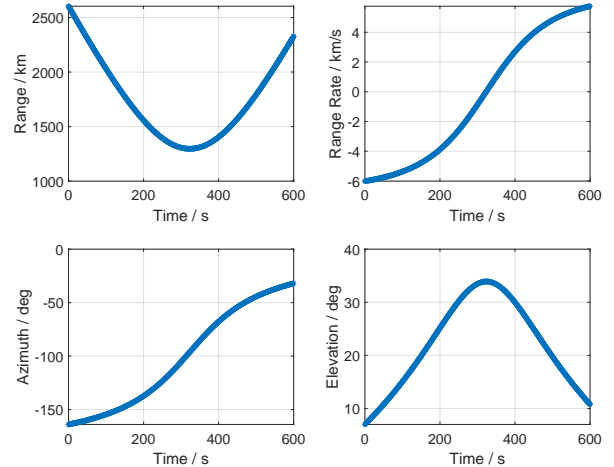


Figure 1: Range, range rate, azimuth and elevation simulated over 600 s.

these n_s data are assigned to the same time instant (the central time of the sub-interval), so that the averaging is a simple arithmetic mean. The accuracy of the averaged observation vector improves according to Eq. 1.

$$\sigma_{av} = \sigma_{raw} / \sqrt{n_s} \quad (1)$$

For linear functions or functions with odd symmetry around the center, the central value is not changed by averaging. To analyse the results, we firstly focused on the impact of the number of samples, trying to understand which is an optimum averaging time interval. Secondly, we investigated the influence of the SNR value in terms of tracking filter performance.

2.2.1. Impact of the number of samples

In this simulation, we took into considerations three different values for n_s to obtain new observation vectors from the raw data: 31, 101 and 401. No weights were applied since all the measurements in the simulation are assumed to have the same SNR of 10 dB.

Figure 3 shows the residuals of the observation vector entries computed as the difference between the nominal trajectory and the averaged data. WGN was added to obtain raw data with a SNR of 10 dB. The corresponding statistics of the residuals (mean, standard deviation and root mean square (RMS)) are listed in Table 2. The same residuals are displayed for the EKF outputs in Figure 4 with the corresponding statistics in Table 3.

If we focus only on the range residuals for the averaging method with 31 and 101 samples, the averaged data seem to perform better than the raw data in both cases (Figure 3a). Nonetheless, while the mean of the average with 31 samples is close to zero, the one with 101 samples is around 11 m. The same behaviour is visible in the EKF range residuals, where the RMS for the observation vectors every 101 samples is the largest. In particular, we

Table 1: TLE used for the performed simulation.

Stella								
1	22824U	93061B	19073.15924862	-.000000030	00000-0	66708-5	0	9990
2	22824	98.9126	48.7284	0006571	13.1848	51.8073	14.27376269326598	

can notice that in the middle of the observation the residuals are higher, while at the beginning and at the end the tracking filter performs better (Figure 4a). The nominal range, shown in Figure 1, is almost linear at the beginning and at the end of the pass, while it is curved in the middle. 31 samples (~ 1 s of sampling time) are enough to better estimate the range parameter, while 101 samples are already too much. It is important to mention that the range is the parameter with the highest variability, therefore the least suitable for a linear fit [3]. By increasing the number of samples to 401, the curvature in the middle becomes clearly visible in the residuals. The mean is ~ 150 m away and it compromises the performance of the tracking filter.

On the other hand, the same discussion does not apply for the range rate and the angle residuals to the same degree. In this case, the statistics of the averaging method with 101 samples are still better than that of the raw data, therefore the averaging technique can be applied for a longer interval of time. Averaging with 401 samples yields still an improvement for the range rate. The angle accuracy instead is lower than the one obtained by the raw data. In Figure 4d we can notice how the residuals increase in the middle of the pass, where the curvature of the nominal elevation is maximal. However, this is not as obvious as on the range.

By considering the state vectors obtained as output of the EKF, it is possible to compute the residuals in the Earth-centered inertial (ECI) reference frame. Figure 4e and Figure 4f show the norm of the position and the velocity vector residuals with respect to the nominal trajectory. In both cases, the averaged data with 31 and 101 pulses are sufficient to approximate the functions since they perform better than the raw data. By using the averaged data with 401 samples instead, the EKF estimates are again poor on the position, especially in the central part. On the other hand, the velocity is well estimated even with such a high revisit rate. This reflects the results obtained on the range rate, the only observation parameter that is well estimated even with 401 samples. We can say that the averaging method works well for a linear function. As soon as a linear function cannot fit the data anymore (i.e. range for long observation time), the performance of the averaging technique degrades. Therefore, averaging with 31 samples is a good choice in this case and we used only this one to perform the experiment on the SNR impact.

2.2.2. Impact of the SNR parameter

After verifying the effective improvement obtained by averaging, we performed another kind of simulation, this

time focusing on the impact of the SNR. For a fixed SNR value, we ran 100 simulations. For each run, we fed the tracking filter with the raw data and the averaged data (31 samples) and we computed the residuals of the observation vectors with respect to the nominal trajectory, and their corresponding RMS. Therefore, it is possible to calculate the RMS of each individual run and to compute the mean of these 100 RMSs. The only quantity changing in every run is the random WGN added to the nominal parameters in order to create the raw data.

Table 4 shows the mean over 100 different runs of the RMS related to the tracking filter residuals. The results are listed for SNR equal to 5 dB, 15 dB, 25 dB and 35 dB. As we can see, at 5 dB the RMS of the averaged data is always lower than the one of the raw data, which means the averaging technique increases the accuracy on all the parameters (range, range rate, azimuth and elevation). This is still true when increasing the SNR to 15 dB. Nevertheless, if we focus on the range, the corresponding mean of the RMS values of the averaged data is lower than the one of the raw data, but only by 0.1 m. In fact, by increasing even more the SNR value to 25 dB, the raw data start outperforming the averaged one, until arriving at 35 dB where the RMS of the raw data is clearly below the one of the averaged data. However, even at 35 dB, the difference between the means of the RMSs is only 0.5 m. It is known that the higher the SNR the higher the accuracy on the measurements. Therefore, by increasing the SNR, the noise added on the simulated measurements decreases having a deeper impact on the raw data in terms of EKF performance. On the other hand, the averaging method performs better on the range rate and on the angles at any SNR value. Again, the range is the most “problematic” parameter to improve with the averaging technique, which is more suitable for linear functions. This assumption is not fulfilled by the range that can be modelled as a quadratic function over a short time interval. [1].

In any case, the results show that, with a low value of SNR, the averaging method completely outperforms the raw data in terms of tracking filter performance. When the SNR is higher we can still say that the averaging technique generally performs better.

2.3. Local filtering technique

Currently, a new technique based on a matched filtering has been developed to improve the accuracy of the pre-processed data [1]. Also in this case, the final observation vectors are computed every 31 pulses. With this filtering technique we are able to compute a new parameter, the range rate rate, that is later used in the EKF in or-

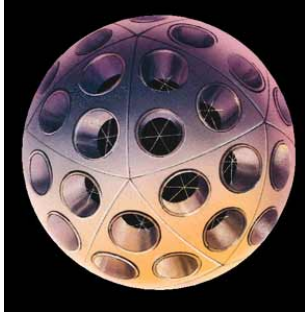


Figure 2: Illustration of the French satellite Stella [CNES]

der to better estimate the state vector of the object. The same simulation described in Section 2.1 (SNR of 10 dB) is used to evaluate the performance of the filtering technique. Figure 5 shows the residuals on the observation vector parameters computed as the difference between the nominal trajectory and the simulated observation vectors. Table 5 lists the statistics related to these residuals. It is obvious how the filtering technique applied to the raw data reduces the noise impact even more than by averaging. Looking at the values of the standard deviation, we can clearly notice how the filtering reduces the σ , especially on the range and range rate. The same results can be observed once these data are processed by means of the EKF. Figure 6 and Table 6 show the EKF residuals and the corresponding statistics, respectively. Also in this case, the highest improvement is on the range and on the range rate. The residuals are lower on the angles too, and consequently on the norm of the ECI position residuals.

3. PERFORMED EXPERIMENTS

In this study, we analyzed three passes of Stella, a French passive satellite launched by CNES in 1993 (Figure 2). Stella is dedicated to geodetic and geophysical studies with Satellite Laser Ranging (SLR). It is a 24 cm diameter sphere covered with 60 identical retroreflectors [4]. The three passes were observed in March 2019 and in this paper we refer to the three different observations with the convention “XXX-YY-ZZ” where XXX is the day of the year (DOY), YY the hour and ZZ the minute of the starting time of the pass. Therefore, the three considered observations are “Stella 073-15-26”, “Stella 077-13-38” and “Stella 077-15-17”. All the passes are really similar to each other, the TIRA system tracked the object for ~ 11 minutes with a maximum elevation around 35-40 degrees. Although Stella is a very small object, high values of the SNR are caused by the high reflectivity due to the presence of specular reflections occurring on the edges of the retroreflectors. In these experiments, we considered a SNR threshold of 13 dB for detection. The choice of these three observations is due to the availability of accurate ephemerides of Stella. For each observation we processed the data according to the three different possibilities and compared the results with the

corresponding ephemerides.

Table 7, Table 8 and Table 9 show the mean, the standard deviation and the RMS of the observation vector residuals and of the norm of position and velocity vector residuals in the ECI frame, as for the simulations. As a first consideration, we can say that the averaging method always outperforms the raw data, exactly like in the simulations. The major improvement is on the standard deviation. Looking at the filtered data, the residuals are always lower in all the passes compared to the raw and the averaged data. The only exception concerns the elevation residuals that are higher in the first and in the third pass. In this case, there is not a total match with the findings of the simulation. Anyway, with real data the accuracy of the position and the velocity estimates is increased by around a factor 2.5, which means that the filtering technique is still guaranteeing the best tracking filter performance.

4. CONCLUSIONS

In this paper, we investigated the performance of tracking filters according to different input data. The EKF was taken as an exemplary tracking filter. Similar results were also achieved with an Unscented Kalman filter. The input data were chosen as raw data or pre-processed data. The idea is to increase the accuracy of the new input data at the cost of a lower revisit rate. In the simulations, we showed that for the averaging method the best performance was obtained by averaging around 31 samples, which means refreshing the observation vector about every second. In addition, the major improvement with respect to the raw data is visible at low SNR, where the raw measurements are more affected by noise. Concerning the filtering technique, the simulated results always outperform the averaged data and the raw data. After the simulations, we tested the algorithms on real data by observing three passes of the French satellite Stella and comparing the EKF results with accurate ephemerides. The averaged data are always more accurate than the raw data, as expected from the simulations. The new filtering technique is always improving the accuracy of almost all the observation parameters and of the position and velocity in the ECI frame.

As a future work, the filtering technique needs to be tested on other objects and with different observation geometries in order to have a better understanding of the parameters that influence the performance of this new method. An investigation of the optimum number of pulses to use in the filtering is needed too. Even if the computational load is higher than a simple average, the simulations show that this method, especially thanks to the range rate parameter, has the potential to improve the accuracy of a tracking filter, more than a simple averaging can do. In the future, the challenge will be to understand if with such a higher computational cost, it is really possible to implement this filtering technique on the raw measurements in real-time before feeding the tracking filter.

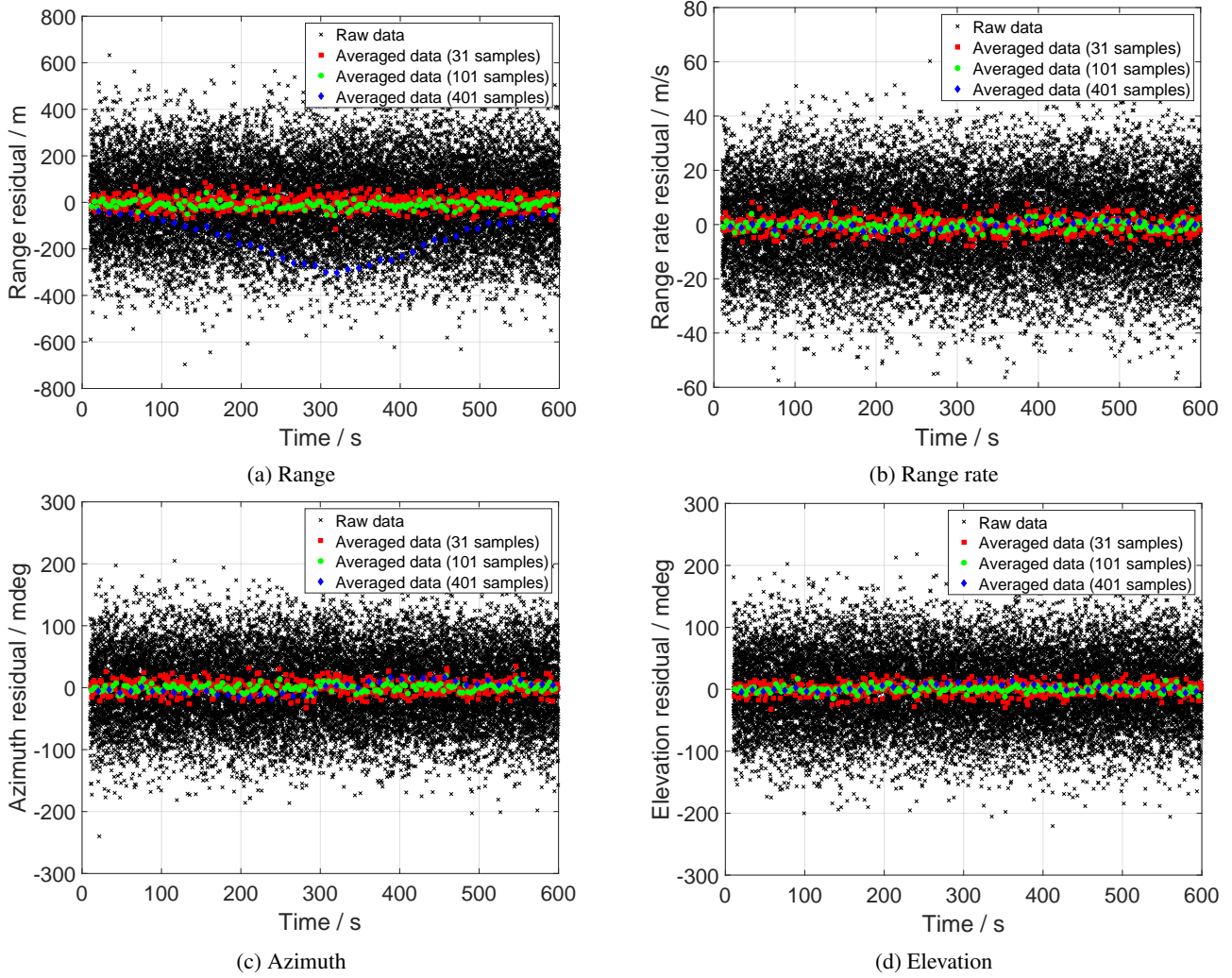
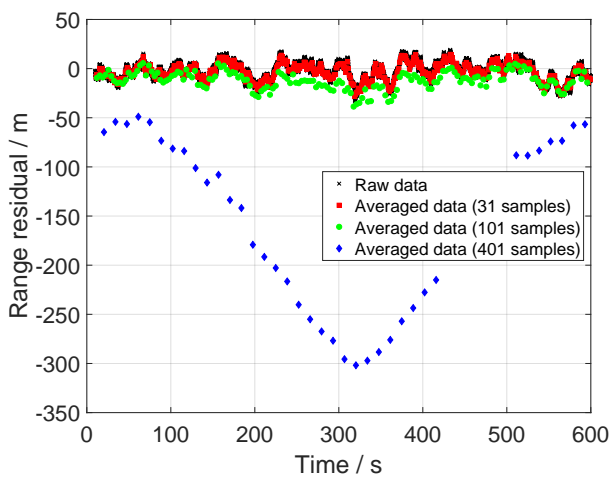


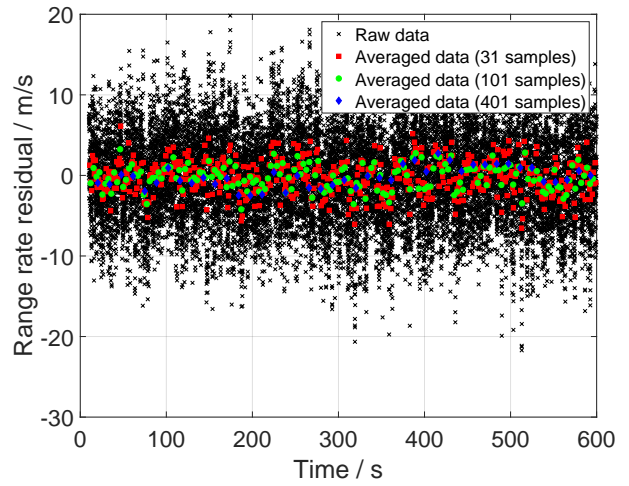
Figure 3: Residuals for the observation vectors, computed as the difference between the nominal trajectory and the simulated observation vectors.

Table 2: Statistics for the residuals of the observation vectors over one run. μ is the mean, σ is the standard deviation and RMS is the root mean square.

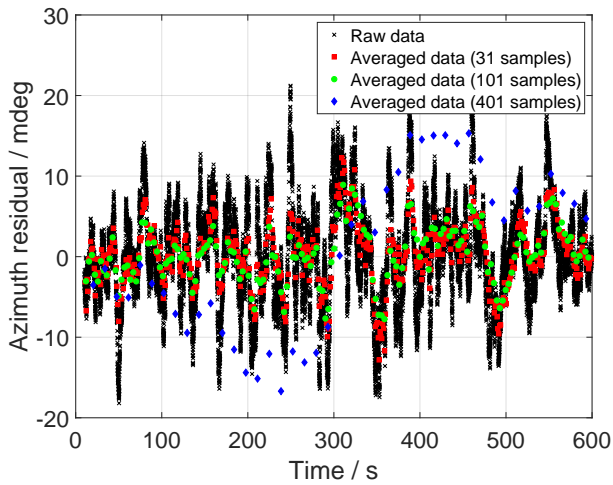
Meas. statistics	Range (m)	Range rate (m/s)	Azimuth (mdeg)	Elevation (mdeg)
Raw data	$\mu = -1.33$ $\sigma = 169.68$ RMS = 169.69	$\mu = 0.07$ $\sigma = 15.73$ RMS = 15.73	$\mu = -0.05$ $\sigma = 57.22$ RMS = 57.22	$\mu = 0.25$ $\sigma = 56.90$ RMS = 56.90
Averaged data (31 samples)	$\mu = -2.25$ $\sigma = 29.50$ RMS = 29.59	$\mu = 0.07$ $\sigma = 2.88$ RMS = 2.88	$\mu = -0.04$ $\sigma = 10.60$ RMS = 10.60	$\mu = 0.26$ $\sigma = 10.15$ RMS = 10.15
Averaged data (101 samples)	$\mu = -11.21$ $\sigma = 17.49$ RMS = 20.73	$\mu = 0.07$ $\sigma = 1.61$ RMS = 1.61	$\mu = -0.04$ $\sigma = 5.89$ RMS = 5.89	$\mu = 0.42$ $\sigma = 5.77$ RMS = 5.77
Averaged data (401 samples)	$\mu = -156.02$ $\sigma = 87.28$ RMS = 178.28	$\mu = 0.05$ $\sigma = 1.35$ RMS = 1.35	$\mu = -0.21$ $\sigma = 9.55$ RMS = 9.55	$\mu = 2.25$ $\sigma = 5.71$ RMS = 6.07



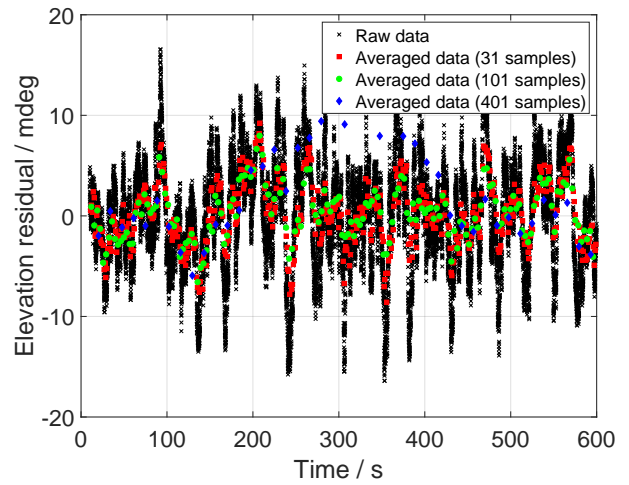
(a) Range



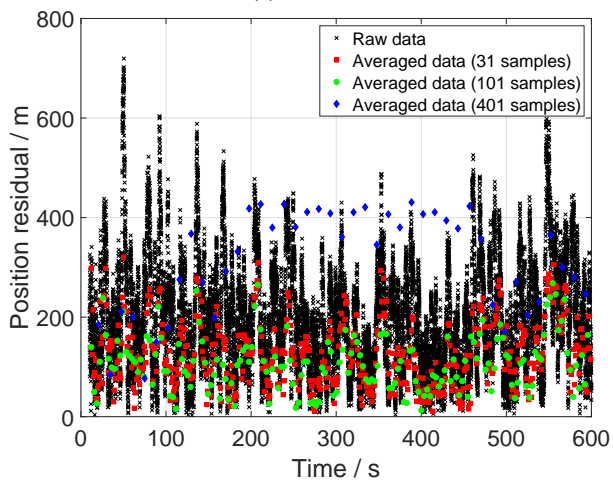
(b) Range rate



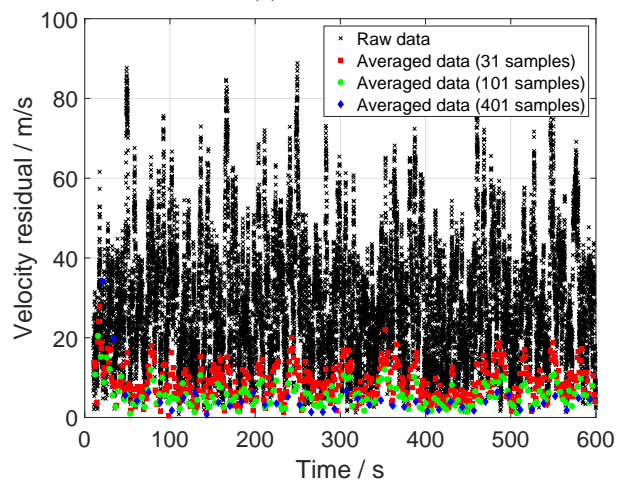
(c) Azimuth



(d) Elevation



(e) Position



(f) Velocity

Figure 4: EKF residuals for the observation vectors (a) - (d) and norm of the position and velocity vector residuals (e) - (f). The residuals are computed as the difference between the nominal trajectory and the tracking filter estimates.

Table 3: Statistics for the EKF residuals over one run. Residuals for the observation vectors and norm of the position and velocity vector residuals. μ is the mean, σ is the standard deviation and RMS is the root mean square.

EKF statistics	Range (m)	Range rate (m/s)	Azimuth (mdeg)	Elevation (mdeg)	Position (m)	Velocity (m/s)
Raw data	$\mu = -0.43$ $\sigma = 11.14$ RMS = 11.15	$\mu = 0.07$ $\sigma = 5.18$ RMS = 5.18	$\mu = -0.02$ $\sigma = 5.41$ RMS = 5.41	$\mu = 0.26$ $\sigma = 5.12$ RMS = 5.13	$\mu = 195.36$ $\sigma = 108.48$ RMS = 223.46	$\mu = 28.65$ $\sigma = 15.08$ RMS = 32.38
Averaged data (31 samples)	$\mu = -1.39$ $\sigma = 10.88$ RMS = 10.96	$\mu = 0.07$ $\sigma = 2.06$ RMS = 2.06	$\mu = 0.03$ $\sigma = 3.38$ RMS = 3.38	$\mu = 0.16$ $\sigma = 3.43$ RMS = 3.43	$\mu = 125.68$ $\sigma = 66.82$ RMS = 142.32	$\mu = 8.56$ $\sigma = 4.28$ RMS = 9.57
Averaged data (101 samples)	$\mu = -10.32$ $\sigma = 12.63$ RMS = 16.28	$\mu = 0.06$ $\sigma = 1.39$ RMS = 1.39	$\mu = 0.07$ $\sigma = 2.84$ RMS = 2.84	$\mu = 0.28$ $\sigma = 2.97$ RMS = 2.97	$\mu = 107.29$ $\sigma = 55.48$ RMS = 120.72	$\mu = 5.70$ $\sigma = 3.11$ RMS = 6.49
Averaged data (401 samples)	$\mu = -156.23$ $\sigma = 87.43$ RMS = 178.53	$\mu = 0.04$ $\sigma = 1.33$ RMS = 1.33	$\mu = 0.04$ $\sigma = 9.30$ RMS = 9.30	$\mu = 2.37$ $\sigma = 5.52$ RMS = 5.94	$\mu = 314.19$ $\sigma = 102.23$ RMS = 330.03	$\mu = 4.75$ $\sigma = 5.43$ RMS = 7.17

Table 4: Statistics for the EKF residuals over 100 runs. For each run the RMS of the residuals is computed. \bar{RMS}_{raw} is the mean of the 100 RMSs for the raw data, \bar{RMS}_{31} is the mean of the 100 RMSs for the averaged data with 31 samples.

EKF statistics	Range (m)	Range rate (m/s)	Azimuth (mdeg)	Elevation (mdeg)
5 dB	$\bar{RMS}_{raw} = 16.87$ $\bar{RMS}_{31} = 16.09$	$\bar{RMS}_{raw} = 6.90$ $\bar{RMS}_{31} = 2.83$	$\bar{RMS}_{raw} = 8.49$ $\bar{RMS}_{31} = 5.63$	$\bar{RMS}_{raw} = 8.25$ $\bar{RMS}_{31} = 5.44$
15 dB	$\bar{RMS}_{raw} = 5.40$ $\bar{RMS}_{31} = 5.31$	$\bar{RMS}_{raw} = 3.85$ $\bar{RMS}_{31} = 1.36$	$\bar{RMS}_{raw} = 3.55$ $\bar{RMS}_{31} = 2.24$	$\bar{RMS}_{raw} = 3.46$ $\bar{RMS}_{31} = 2.22$
25 dB	$\bar{RMS}_{raw} = 1.70$ $\bar{RMS}_{31} = 1.98$	$\bar{RMS}_{raw} = 2.02$ $\bar{RMS}_{31} = 0.50$	$\bar{RMS}_{raw} = 1.49$ $\bar{RMS}_{31} = 0.92$	$\bar{RMS}_{raw} = 1.45$ $\bar{RMS}_{31} = 0.89$
35 dB	$\bar{RMS}_{raw} = 0.73$ $\bar{RMS}_{31} = 1.26$	$\bar{RMS}_{raw} = 1.02$ $\bar{RMS}_{31} = 0.20$	$\bar{RMS}_{raw} = 0.63$ $\bar{RMS}_{31} = 0.37$	$\bar{RMS}_{raw} = 0.61$ $\bar{RMS}_{31} = 0.36$

Table 5: Statistics for the residuals of the observation vectors over one run. μ is the mean, σ is the standard deviation and RMS is the root mean square.

Meas. statistics	Range (m)	Range rate (m/s)	Azimuth (mdeg)	Elevation (mdeg)
Raw data	$\mu = 1.09$ $\sigma = 170.33$ RMS = 170.33	$\mu = 0.04$ $\sigma = 15.75$ RMS = 15.75	$\mu = 0.59$ $\sigma = 56.75$ RMS = 56.75	$\mu = -0.04$ $\sigma = 57.02$ RMS = 57.02
Averaged data (31 samples)	$\mu = 0.15$ $\sigma = 30.27$ RMS = 30.27	$\mu = 0.05$ $\sigma = 2.83$ RMS = 2.83	$\mu = 0.59$ $\sigma = 10.65$ RMS = 10.65	$\mu = -0.04$ $\sigma = 9.98$ RMS = 9.98
Filtered data	$\mu = 1.02$ $\sigma = 13.29$ RMS = 13.31	$\mu = 0.01$ $\sigma = 0.01$ RMS = 0.01	$\mu = 0.55$ $\sigma = 4.60$ RMS = 4.62	$\mu = -0.38$ $\sigma = 4.24$ RMS = 4.26

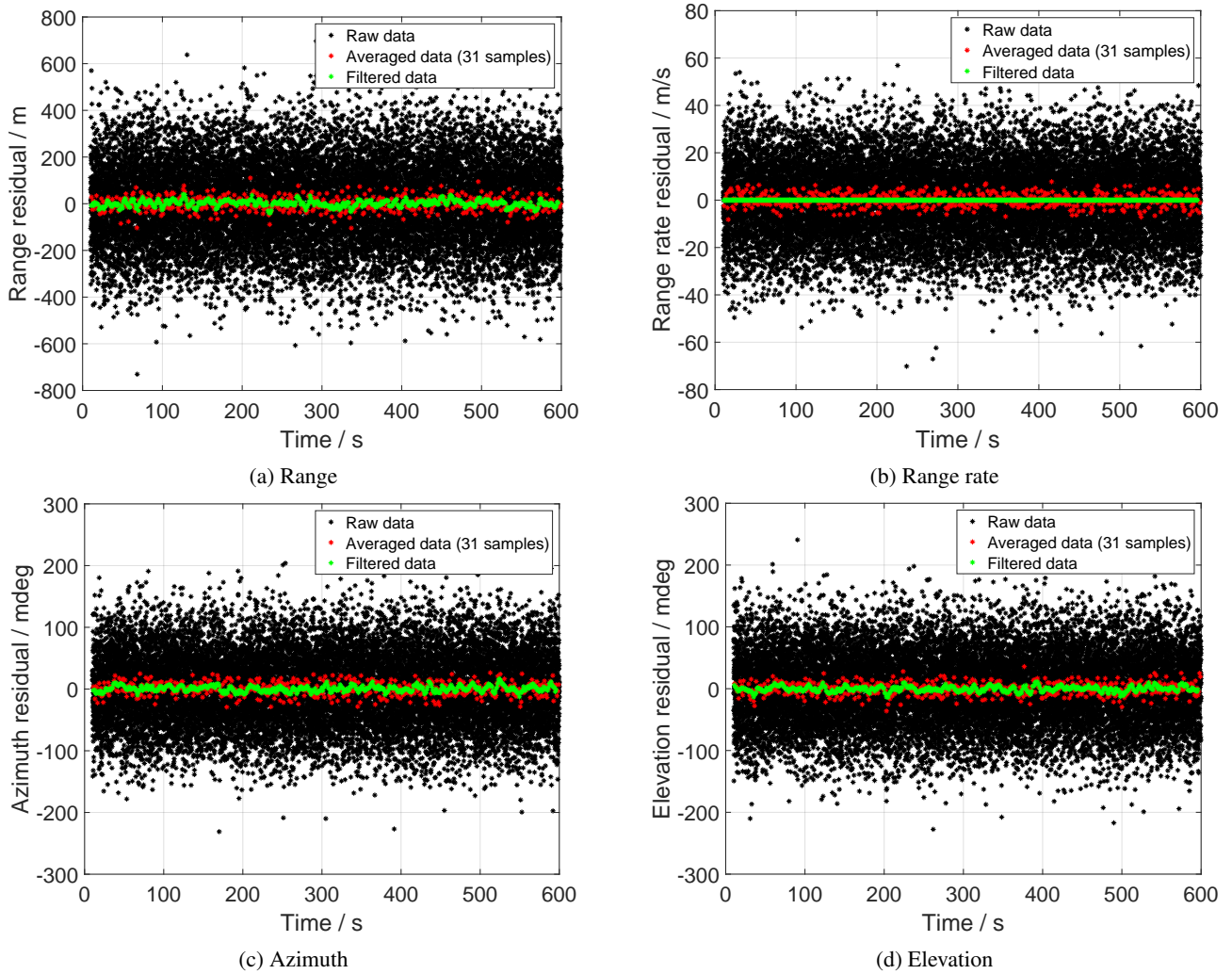
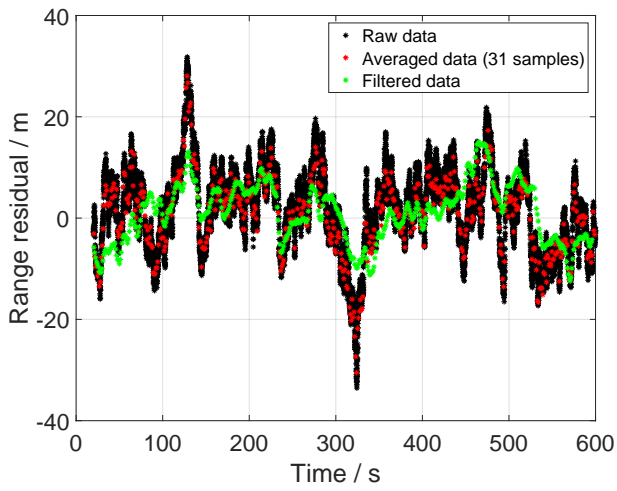


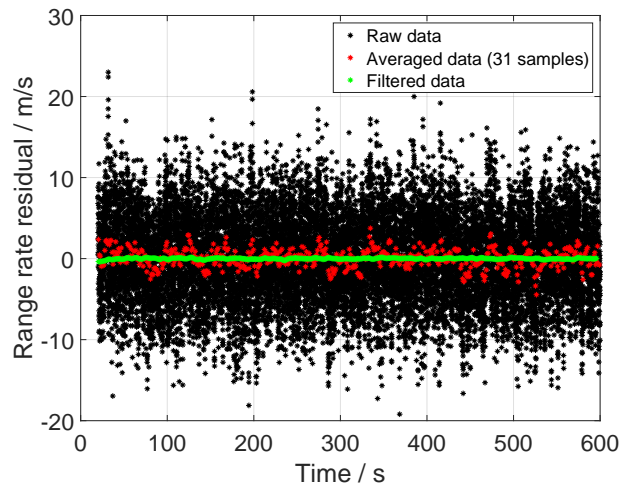
Figure 5: Residuals for the observation vectors, computed as the difference between the nominal trajectory and the simulated observation vectors.

Table 6: Statistics for the EKF residuals over one run. Residuals for the observation vectors and norm of the position and velocity vector residuals. μ is the mean, σ is the standard deviation and RMS is the root mean square.

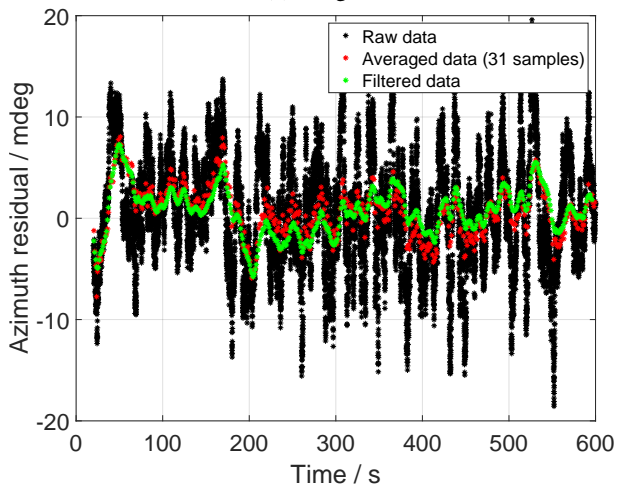
EKF statistics	Range (m)	Range rate (m/s)	Azimuth (mdeg)	Elevation (mdeg)	Position (m)	Velocity (m/s)
Raw data	$\mu = 1.34$ $\sigma = 8.37$ RMS = 8.48	$\mu = 0.04$ $\sigma = 5.22$ RMS = 5.22	$\mu = 0.64$ $\sigma = 5.46$ RMS = 5.49	$\mu = -0.11$ $\sigma = 4.94$ RMS = 4.94	$\mu = 190.43$ $\sigma = 106.09$ RMS = 217.99	$\mu = 27.83$ $\sigma = 13.37$ RMS = 30.87
Averaged data (31 samples)	$\mu = 0.43$ $\sigma = 7.85$ RMS = 7.86	$\mu = 0.03$ $\sigma = 1.17$ RMS = 1.17	$\mu = 0.67$ $\sigma = 2.58$ RMS = 2.66	$\mu = -0.92$ $\sigma = 2.59$ RMS = 2.61	$\mu = 99.66$ $\sigma = 73.48$ RMS = 123.78	$\mu = 4.74$ $\sigma = 6.60$ RMS = 8.12
Filtered data	$\mu = 0.31$ $\sigma = 5.59$ RMS = 5.75	$\mu = 0.01$ $\sigma = 0.06$ RMS = 0.06	$\mu = 0.79$ $\sigma = 2.25$ RMS = 2.38	$\mu = -0.56$ $\sigma = 2.28$ RMS = 2.35	$\mu = 84.00$ $\sigma = 69.95$ RMS = 109.27	$\mu = 3.52$ $\sigma = 6.31$ RMS = 7.22



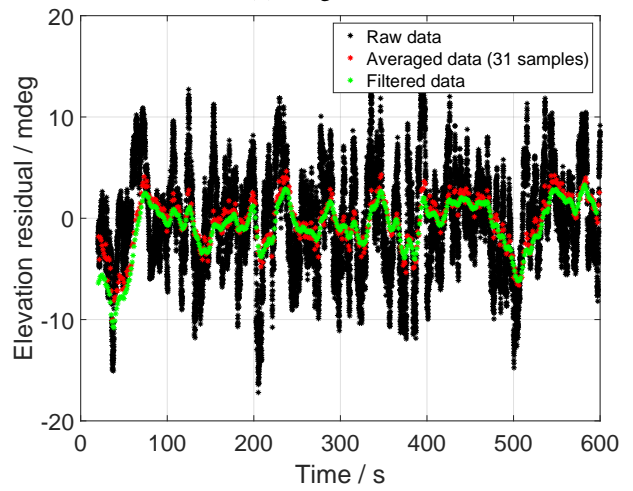
(a) Range



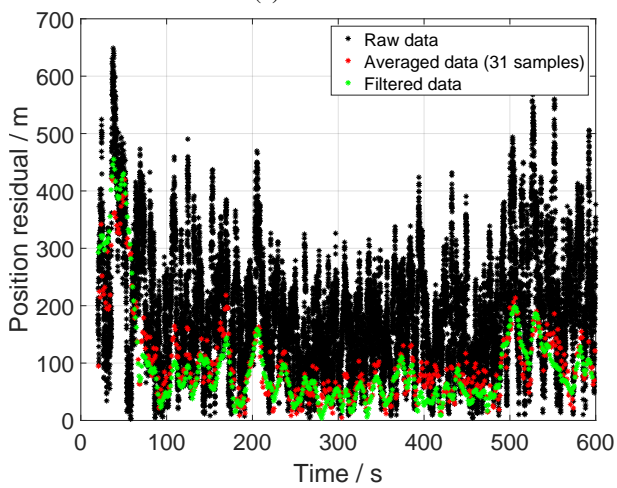
(b) Range rate



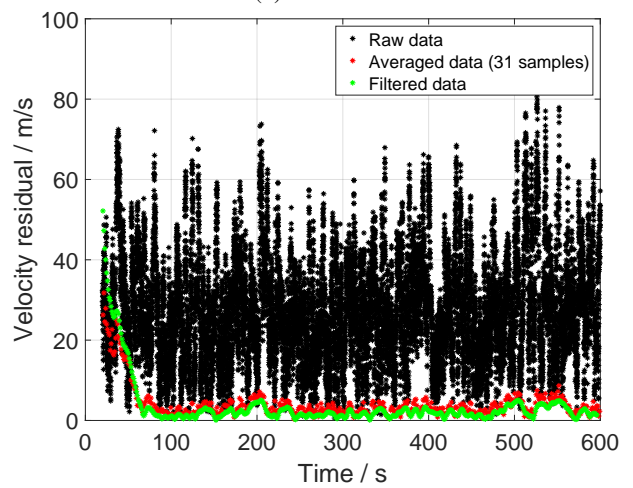
(c) Azimuth



(d) Elevation



(e) Position



(f) Velocity

Figure 6: EKF residuals for the observation vectors (a) - (d) and norm of the position and velocity vector residuals (e) - (f). The residuals are computed as the difference between the nominal trajectory and the tracking filter estimates.

Table 7: Statistics for the EKF residuals of the observation Stella 073-15-26. Residuals for the observation vectors and norm of the position and velocity vector residuals. μ is the mean, σ is the standard deviation and RMS is the root mean square.

Stella 073-15-26 EKF statistics	Range (m)	Range rate (m/s)	Azimuth (mdeg)	Elevation (mdeg)	Position (m)	Velocity (m/s)
Raw data	$\mu = -3.35$ $\sigma = 6.06$ RMS = 6.93	$\mu = 0.08$ $\sigma = 2.11$ RMS = 2.11	$\mu = 9.83$ $\sigma = 1.67$ RMS = 9.97	$\mu = -3.04$ $\sigma = 2.29$ RMS = 3.80	$\mu = 254.31$ $\sigma = 52.05$ RMS = 259.58	$\mu = 4.25$ $\sigma = 2.16$ RMS = 4.77
Averaged data (31 samples)	$\mu = -3.86$ $\sigma = 4.31$ RMS = 5.78	$\mu = 0.11$ $\sigma = 1.21$ RMS = 1.22	$\mu = 9.81$ $\sigma = 1.54$ RMS = 9.93	$\mu = -3.07$ $\sigma = 1.68$ RMS = 3.50	$\mu = 251.61$ $\sigma = 38.98$ RMS = 254.61	$\mu = 2.67$ $\sigma = 1.14$ RMS = 2.90
Filtered data	$\mu = -2.84$ $\sigma = 2.12$ RMS = 3.54	$\mu = -0.01$ $\sigma = 0.17$ RMS = 0.17	$\mu = 0.34$ $\sigma = 1.25$ RMS = 1.30	$\mu = -3.83$ $\sigma = 1.45$ RMS = 4.09	$\mu = 106.99$ $\sigma = 30.01$ RMS = 111.11	$\mu = 1.71$ $\sigma = 0.82$ RMS = 1.89

Table 8: Statistics for the EKF residuals of the observation Stella 077-13-38. Residuals for the observation vectors and norm of the position and velocity vector residuals. μ is the mean, σ is the standard deviation and RMS is the root mean square.

Stella 077-13-38 EKF statistics	Range (m)	Range rate (m/s)	Azimuth (mdeg)	Elevation (mdeg)	Position (m)	Velocity (m/s)
Raw data	$\mu = -5.59$ $\sigma = 9.00$ RMS = 10.59	$\mu = 0.10$ $\sigma = 2.08$ RMS = 2.09	$\mu = 8.28$ $\sigma = 2.31$ RMS = 8.60	$\mu = 1.92$ $\sigma = 2.63$ RMS = 3.26	$\mu = 221.09$ $\sigma = 95.29$ RMS = 240.75	$\mu = 4.98$ $\sigma = 2.91$ RMS = 5.77
Averaged data (31 samples)	$\mu = -5.79$ $\sigma = 8.10$ RMS = 9.95	$\mu = 0.12$ $\sigma = 1.19$ RMS = 1.20	$\mu = 8.25$ $\sigma = 2.25$ RMS = 8.55	$\mu = 1.84$ $\sigma = 2.20$ RMS = 2.87	$\mu = 216.49$ $\sigma = 81.56$ RMS = 231.32	$\mu = 3.27$ $\sigma = 1.67$ RMS = 3.68
Filtered data	$\mu = -4.78$ $\sigma = 6.96$ RMS = 8.43	$\mu = 0.00$ $\sigma = 0.24$ RMS = 0.24	$\mu = -1.47$ $\sigma = 3.01$ RMS = 3.34	$\mu = 1.06$ $\sigma = 1.78$ RMS = 2.07	$\mu = 82.38$ $\sigma = 44.23$ RMS = 93.43	$\mu = 1.96$ $\sigma = 0.96$ RMS = 2.18

Table 9: Statistics for the EKF residuals of the observation Stella 077-15-17. Residuals for the observation vectors and norm of the position and velocity vector residuals. μ is the mean, σ is the standard deviation and RMS is the root mean square.

Stella 077-15-17 EKF statistics	Range (m)	Range rate (m/s)	Azimuth (mdeg)	Elevation (mdeg)	Position (m)	Velocity (m/s)
Raw data	$\mu = -4.81$ $\sigma = 6.94$ RMS = 8.44	$\mu = 0.09$ $\sigma = 2.09$ RMS = 2.10	$\mu = 8.74$ $\sigma = 1.88$ RMS = 8.94	$\mu = -2.52$ $\sigma = 2.38$ RMS = 3.46	$\mu = 208.52$ $\sigma = 69.17$ RMS = 219.70	$\mu = 4.44$ $\sigma = 2.19$ RMS = 4.95
Averaged data (31 samples)	$\mu = -5.13$ $\sigma = 5.33$ RMS = 7.39	$\mu = 0.14$ $\sigma = 1.13$ RMS = 1.14	$\mu = 8.73$ $\sigma = 1.69$ RMS = 8.90	$\mu = -2.57$ $\sigma = 1.93$ RMS = 3.21	$\mu = 207.91$ $\sigma = 59.66$ RMS = 216.28	$\mu = 2.88$ $\sigma = 1.39$ RMS = 3.19
Filtered data	$\mu = -4.23$ $\sigma = 2.51$ RMS = 4.92	$\mu = -0.01$ $\sigma = 0.20$ RMS = 0.20	$\mu = -0.85$ $\sigma = 1.31$ RMS = 1.56	$\mu = -3.30$ $\sigma = 1.57$ RMS = 3.66	$\mu = 86.88$ $\sigma = 25.54$ RMS = 90.55	$\mu = 1.75$ $\sigma = 0.91$ RMS = 1.97

REFERENCES

1. Cerutti-Maori D. et al., (Apr 2021). *A novel High-Precision Observation Mode for the Tracking and Imaging Radar TIRA – Principle and Performance Evaluation*, 8th European Conference on Space Debris, ESA/ESOC, Darmstadt, Germany, Virtual Conference
2. Schmidt S.F., McGee L.A., (1961). *Discovery of the Kalman Filter as a Practical Tool for Aerospace and Industry*, NASA report nr. TM-86847, Ames Research Center, Moffet Field CA 94035, National Aeronautics and Space Administration, Washington, DC 20546
3. Kaiser H., Jehn R., (1996). *Determination of Rough Orbital Elements From Radar Data in Beam-Park Mode*, European Space Agency, European Space Operations Center, Mission Operations Department, Mission Analysis Section, ESOC Robert-Bosch-Str. 5, 64293 Darmstadt, Germany
4. eoPortal Directory ESA, (2000-2019). <https://directory.eoportal.org/web/eoportal/satellite-missions/s/starlette>, Starlette, eoPortal Directory, Satellite Missions, ESA